

## ***Electronic Supporting Information (ESI)***

### **Protonation-induced self-assembly of bis-phenanthroline macrocycles into nanofibers arrayed with tetrachloroaurate, hexachloroplatinate, or phosphorolybdate ions**

Shohei Tashiro,\* Shun Shimizu, Masumi Kuritani, and Mitsuhiko Shionoya\*

*Department of Chemistry, Graduate School of Science, The University of Tokyo, 7-3-1 Hongo,  
Bunkyo-ku, Tokyo 113-0033, Japan*

• <b>Materials and methods</b>	page S2
• <b>Reaction of 1 and H<sub>AuCl<sub>4</sub>·4H<sub>2</sub>O</sub></b>	page S3
• <b>Reaction of 2 and H<sub>AuCl<sub>4</sub>·4H<sub>2</sub>O</sub></b>	page S8
• <b>Reaction of 1 and H<sub>2</sub>PtCl<sub>6</sub>·6H<sub>2</sub>O</b>	page S11
• <b>Reaction of 2 and H<sub>2</sub>PtCl<sub>6</sub>·6H<sub>2</sub>O</b>	page S15
• <b>Reaction of 1 and H<sub>3</sub>PMo<sub>12</sub>O<sub>40</sub>·nH<sub>2</sub>O</b>	page S16
• <b>Reaction of 2 and H<sub>3</sub>PMo<sub>12</sub>O<sub>40</sub>·nH<sub>2</sub>O</b>	page S20
• <b>Reduction of nanofibers composed of 1 and H<sub>AuCl<sub>4</sub>·4H<sub>2</sub>O</sub></b>	page S21
• <b>Reduction of nanofibers composed of 1 and H<sub>3</sub>PMo<sub>12</sub>O<sub>40</sub>·nH<sub>2</sub>O</b>	page S22
• <b>References</b>	page S23

## **Materials and methods**

Macrocyclic **1** and 2,9-diphenyl-1,10-phenanthroline (**2**) were prepared according to our previous report.<sup>1</sup> Chlorinated solvent CHCl<sub>3</sub> or CDCl<sub>3</sub> was treated with activated basic alumina to exclude the influence of hydrogen chloride. Other solvents, organic and inorganic reagents, substrates are commercially available, and were used without further purification.

NMR spectroscopic measurement was performed using a Bruker AVANCE 500 spectrometer, and <sup>1</sup>H NMR spectra were calibrated based on the signal of Si(CH<sub>3</sub>)<sub>4</sub> (0 ppm). UV-vis spectroscopy was performed using a HITACHI U-3500 or a JASCO V-770 spectrophotometers. Atomic force microscope (AFM) images in dry-states were observed on an SII SPI4000 probe station with an SPA300HV unit using a DFM mode. Transmission electron microscope (TEM) images, scanning TEM (STEM) images and energy dispersive X-ray spectroscopy (EDS) mapping were obtained using a JEOL JEM-2100F microscope without staining. DLS measurements were performed using an OTSUKA ELECTRONICS DLS8000 instrument equipped with a He-Ne laser (633 nm wavelength). Electrospray ionization-time-of-flight (ESI-TOF) mass spectra were recorded on a Waters LCT Premier XE spectrometer. Single-crystal X-ray diffraction (XRD) analyses were performed using a Rigaku RAXIS-RAPID imaging plate diffractometer with MoK $\alpha$  radiation, and the obtained data were analyzed using a CrystalStructure crystallographic software package except for refinement, which was performed using SHELXL-2013 program suite.<sup>2</sup> X-ray structures were displayed using a Mercury program. Powder XRD analyses were performed using a Rigaku XtaLAB P200 diffractometer with CuK $\alpha$  radiation.

## Reaction of 1 and H<sub>2</sub>AuCl<sub>4</sub>·4H<sub>2</sub>O

Concentration of **1** in a solution was determined by <sup>1</sup>H NMR measurement with anisole as an internal standard. Concentration of H<sub>2</sub>AuCl<sub>4</sub>·4H<sub>2</sub>O was determined by UV-vis absorption measurement according to a reference ( $\epsilon_{287(\text{water})} = 3,133 \text{ L} \cdot \text{mol}^{-1} \cdot \text{cm}^{-1}$ ).<sup>3</sup>

### • ESI-TOF mass analysis

A CH<sub>3</sub>CN solution of H<sub>2</sub>AuCl<sub>4</sub>·4H<sub>2</sub>O (1.88 mM, 53  $\mu$ L, 2.0 equiv.) was added to a solution of **1** (100  $\mu$ M, 500  $\mu$ L, CHCl<sub>3</sub>/CH<sub>3</sub>CN = 10/1) to conduct ESI-TOF mass measurement.

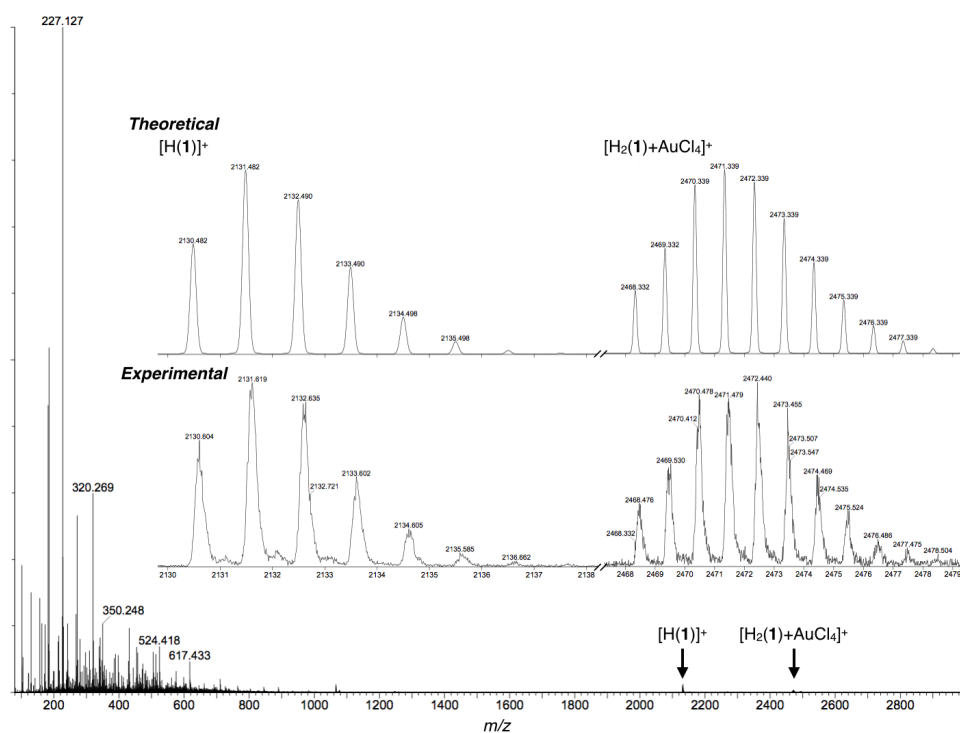


Figure S1. ESI-TOF mass spectrum of a 1:2 mixture of **1** and H<sub>2</sub>AuCl<sub>4</sub>·4H<sub>2</sub>O (CHCl<sub>3</sub>/CH<sub>3</sub>CN = 10/1)

• <sup>1</sup>H NMR analysis

A CD<sub>3</sub>CN solution of H<sub>2</sub>AuCl<sub>4</sub>·4H<sub>2</sub>O (1.81 mM) was added stepwise to a solution of **1** (84 μM, 1.0 mL, CDCl<sub>3</sub>/CD<sub>3</sub>CN = 10/1, containing 84 μM anisole as an internal standard), followed by <sup>1</sup>H NMR measurement. This operation was repeated until a total amount of the added H<sub>2</sub>AuCl<sub>4</sub> reached 4.0 equiv. No signals of cleaved benzyl ether groups of **1** were observed during this experiment, which ensured stability of **1** under this condition even in the presence of 4 equiv. of H<sub>2</sub>AuCl<sub>4</sub>.

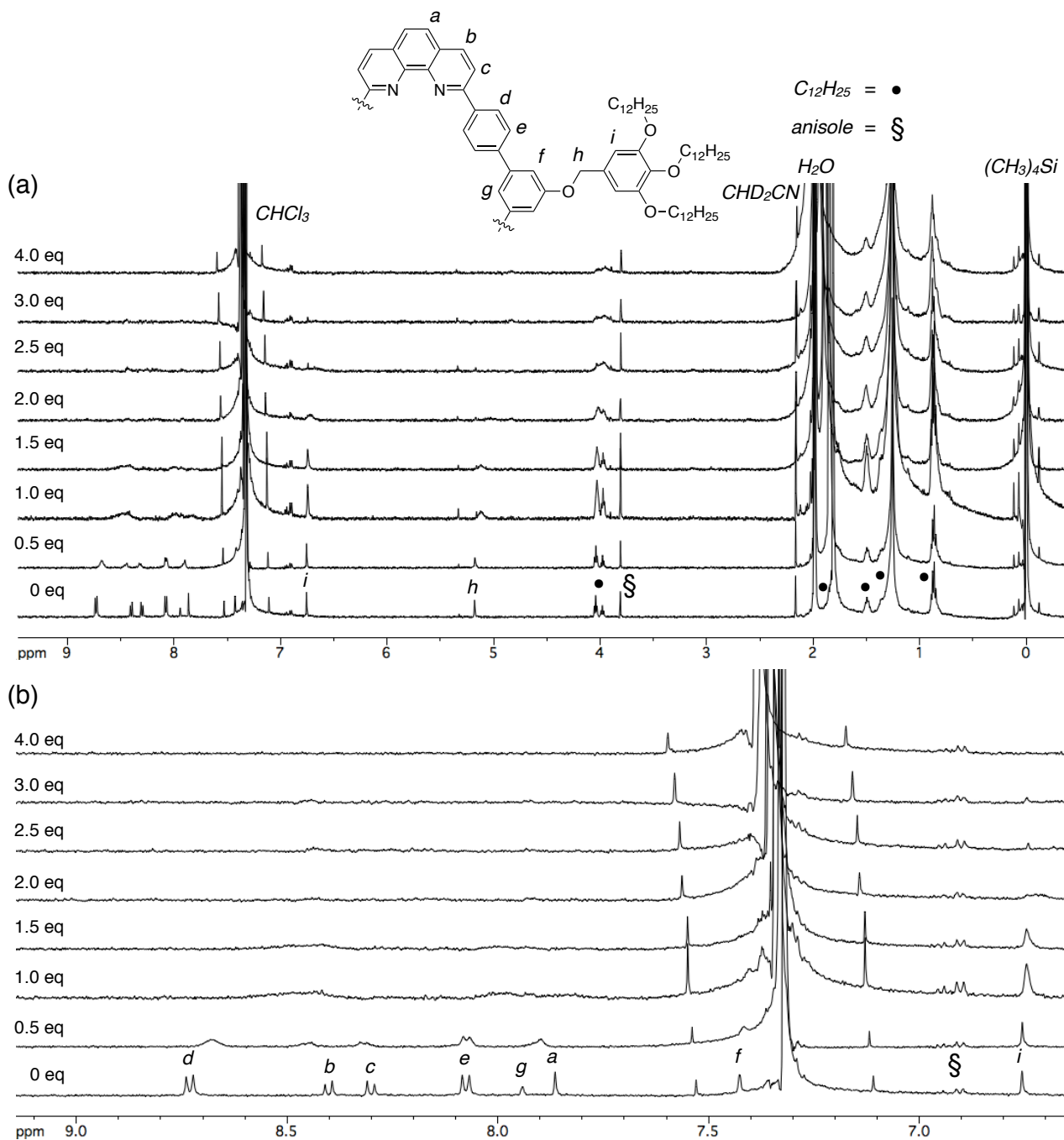


Figure S2. <sup>1</sup>H NMR spectra (whole region (a) and aromatic region (b)) of **1** with different equivalents of H<sub>2</sub>AuCl<sub>4</sub>·4H<sub>2</sub>O (500 MHz, CDCl<sub>3</sub>/CD<sub>3</sub>CN = 10/1, 27 °C, [**1**] = 84 μM, containing anisole as an internal standard)

• *UV-vis analysis*

A CH<sub>3</sub>CN solution of HAuCl<sub>4</sub>·4H<sub>2</sub>O (2.90 mM) was added stepwise to a solution of **1** (29 μM, 4.0 mL, CHCl<sub>3</sub>/CH<sub>3</sub>CN = 10/1), followed by UV-vis absorption measurement. This operation was repeated until a total amount of the added HAuCl<sub>4</sub> reached 10 equiv. The significant increase in absorption intensity around 330 nm after adding more than 2.25 equiv. of HAuCl<sub>4</sub> can be ascribed to the presence of free HAuCl<sub>4</sub> molecules (Figure S4).

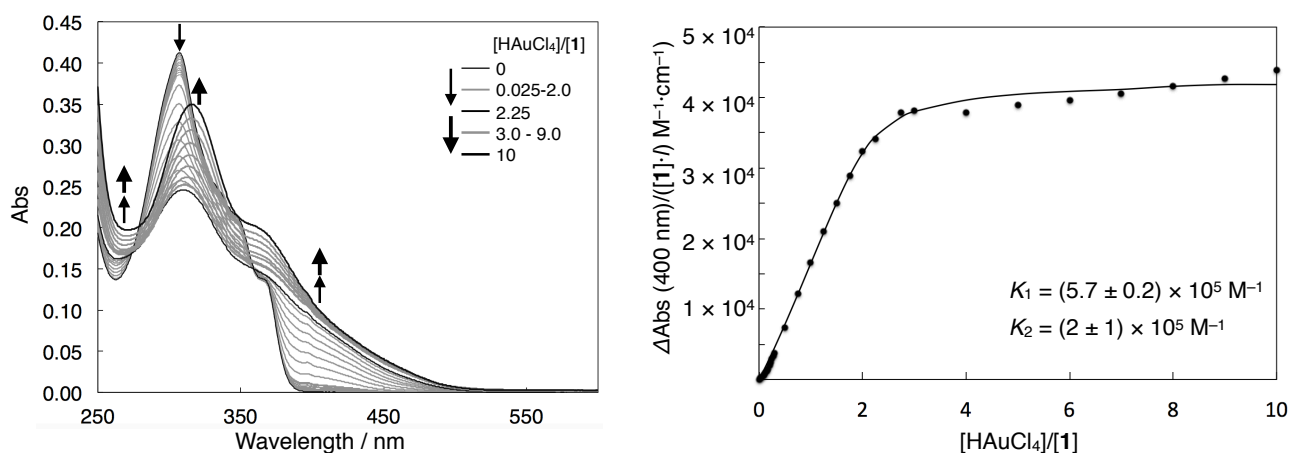
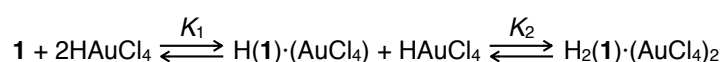


Figure S3. UV-vis spectra of **1** with different equivalents of HAuCl<sub>4</sub>·4H<sub>2</sub>O (CHCl<sub>3</sub>/CH<sub>3</sub>CN = 10/1, 20 °C, [1] = 29 μM, *l* = 0.1 cm) and apparent protonation constant analysis by the least-square fitting to the absorption change  $\Delta$ Abs at 400 nm (solid circle: observed; line: calculated). The simulated curve is calculated based on the theoretical absorption of species mentioned in the equation below including free HAuCl<sub>4</sub>.

The apparent protonation constants  $K_1$  and  $K_2$  are defined as follows.



$$K_1 = \frac{[\text{H}(\mathbf{1}) \cdot (\text{AuCl}_4)]}{[\mathbf{1}][\text{HAuCl}_4]}$$

$$K_2 = \frac{[\text{H}_2(\mathbf{1}) \cdot (\text{AuCl}_4)_2]}{[\text{H}(\mathbf{1}) \cdot (\text{AuCl}_4)][\text{HAuCl}_4]}$$

The error of each constant  $\delta K_1$  and  $\delta K_2$  are calculated from the cell length *l* and the initial concentration of the macrocycle [1]<sub>0</sub> by the least-square fitting above according to the following equations.

$$\delta K = \frac{1}{\sqrt{n}} \sqrt{\frac{1}{n-1} \sum_i^n \left( \frac{\partial K}{\partial [1]} \frac{\partial [1]}{\partial \Delta \varepsilon} + \frac{\partial K}{\partial [\text{HAuCl}_4]} \frac{\partial [\text{HAuCl}_4]}{\partial \Delta \varepsilon} \right)^2 (\delta \Delta \varepsilon)^2}$$

Where:

$$\Delta\varepsilon = \frac{\Delta Abs}{[1]_0 \cdot l}$$

Disagreement between the observed and the calculated  $\Delta Abs$  values after adding more than 2.25 equiv. of  $\text{HAuCl}_4$  indicates the formation of another species such as larger round aggregates observed in AFM analysis of a sample containing excess amount of  $\text{HAuCl}_4$  (Figure S6d).

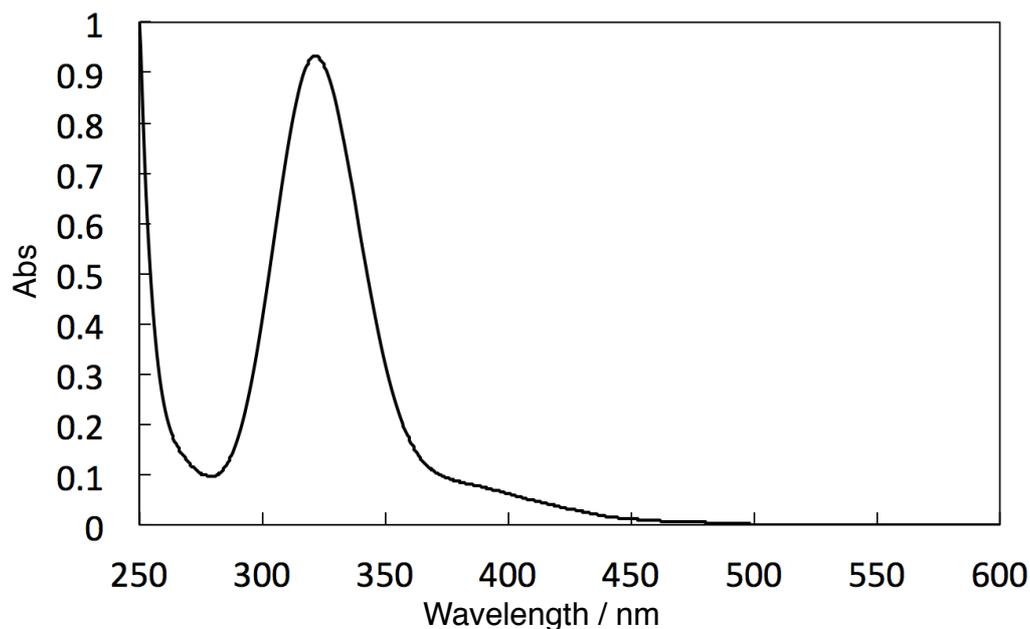
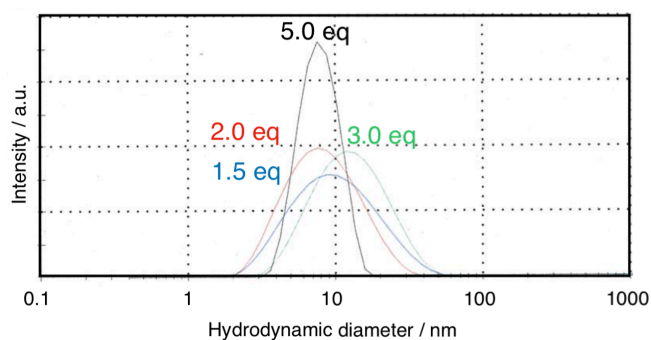


Figure S4. UV-vis spectrum of  $\text{H[AuCl}_4\text{]}\cdot 4\text{H}_2\text{O}$  ( $\text{CHCl}_3/\text{CH}_3\text{CN} = 10/1$ ,  $20\text{ }^\circ\text{C}$ ,  $164\text{ }\mu\text{M}$ ,  $l = 1\text{ cm}$ )

• *DLS analysis*

A solution of  $\text{H[AuCl}_4\text{]}\cdot 4\text{H}_2\text{O}$  (22.9 mM for 1.0 equiv.; 34.4 mM for 1.5 equiv.; 45.8 mM for 2.0 equiv.; 68.7 mM for 3.0 equiv.; 115 mM for 5.0 equiv., 26  $\mu\text{L}$ ) was added to a solution of **1** (120  $\mu\text{M}$ , 5.0 mL) in  $\text{CHCl}_3/\text{CH}_3\text{CN}$  (10/1) and DLS was then measured.



$[\text{H[AuCl}_4\text{]}/[\mathbf{1}]]$	Z-Average (nm)	PdI
$\leq 1.0$	Not detectable	
1.5	9.77	0.259
2.0	7.17	0.206
3.0	11.2	0.240
5.0	8.20	0.204

Figure S5. DLS analysis of a  $\text{CHCl}_3/\text{CH}_3\text{CN}$  (10/1) solution of **1** with 1.5 equiv. (blue trace), 2.0 equiv. (red trace), 3.0 equiv. (green trace) and 5.0 equiv. (black trace) of  $\text{H[AuCl}_4\text{]}\cdot 4\text{H}_2\text{O}$

- *AFM analysis*

A CH<sub>3</sub>CN solution of H<sub>2</sub>AuCl<sub>4</sub>·4H<sub>2</sub>O (1.81 mM, 56.4 μL, 2.0 equiv.; 2.72 mM, 56.4 μL, 3.0 equiv.; 3.62 mM, 56.4 μL, 4.0 equiv.) was added to a CHCl<sub>3</sub> solution of **1** (102 μM, 500 μL). Right after 10-fold dilution with CHCl<sub>3</sub>/CH<sub>3</sub>CN = 10/1, the solution was spin-coated on mica to conduct AFM measurement.

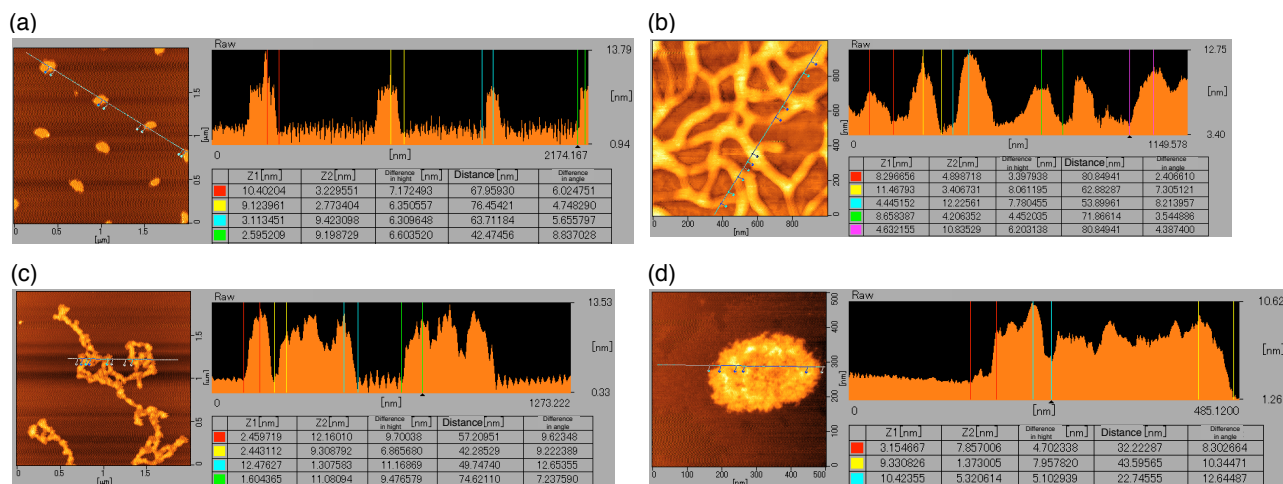


Figure S6. Dry-state AFM images of **1** with (a) 0 equiv., (b) 2 equiv., (c) 3 equiv. and (d) 4 equiv. of H<sub>2</sub>AuCl<sub>4</sub>·4H<sub>2</sub>O on mica

- *STEM-EDS analysis*

A CH<sub>3</sub>CN solution of H<sub>2</sub>AuCl<sub>4</sub>·4H<sub>2</sub>O (2.07 mM, 100 μL, 1.9 equiv.) was added to a CHCl<sub>3</sub> solution of **1** (109 μM, 1.0 mL). Right after dilution to 30 μM with CHCl<sub>3</sub>/CH<sub>3</sub>CN = 10/1, the solution was drop-cast on a carbon-coated Cu grid to conduct STEM and EDS measurement.

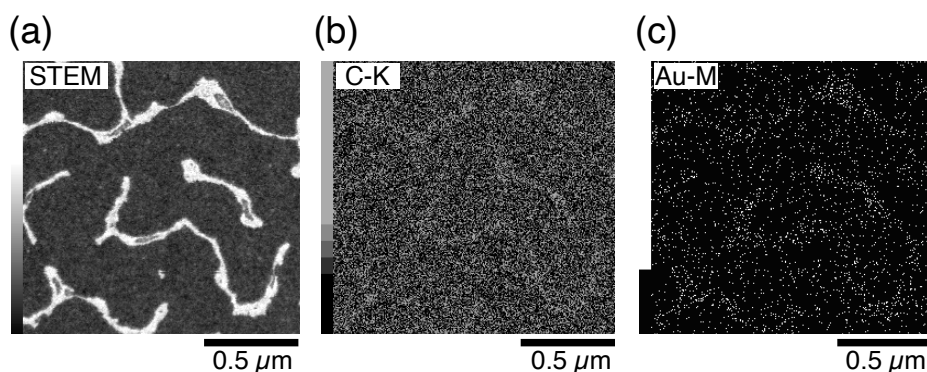


Figure S7. (a) A dark-field STEM image and color-corrected EDS maps for (b) C (K-peak) and (c) Au (M-peak) of nanofibers composed of **1** and Au.

- *PXRD analysis*

A CH<sub>3</sub>CN solution of H<sub>2</sub>AuCl<sub>4</sub>·4H<sub>2</sub>O (1.88 mM, 530 μL, 2.0 equiv.) was added to a CHCl<sub>3</sub>

solution of **1** (100  $\mu$ M, 5.0 mL). The mixture was slowly evaporated on a capillary glass tube to conduct powder X-ray diffraction analysis.

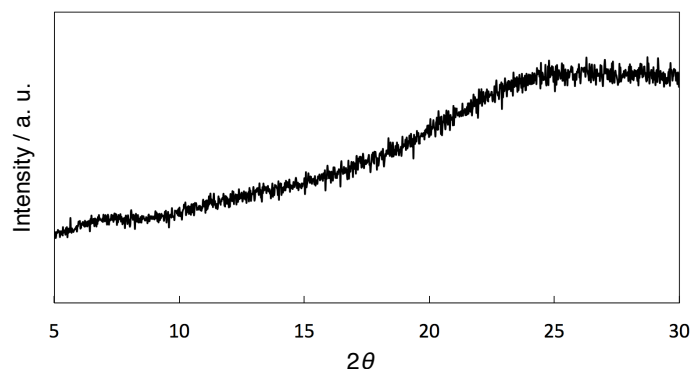


Figure S8. PXRD pattern of a solid obtained by evaporating a mixture of **1** and  $\text{HAuCl}_4 \cdot 4\text{H}_2\text{O}$  in  $\text{CHCl}_3/\text{CH}_3\text{CN}$  (10:1)

### Reaction of **2** and $\text{HAuCl}_4 \cdot 4\text{H}_2\text{O}$

#### • $^1\text{H}$ NMR analysis

A  $\text{CD}_3\text{CN}$  solution of  $\text{HAuCl}_4 \cdot 4\text{H}_2\text{O}$  (5.3 mM) was added stepwise to a solution of **2** (100  $\mu$ M, 1.0 mL,  $\text{CDCl}_3$ ), followed by  $^1\text{H}$  NMR measurement. This operation was repeated until a total amount of the added  $\text{HAuCl}_4$  reached 5.0 equiv.

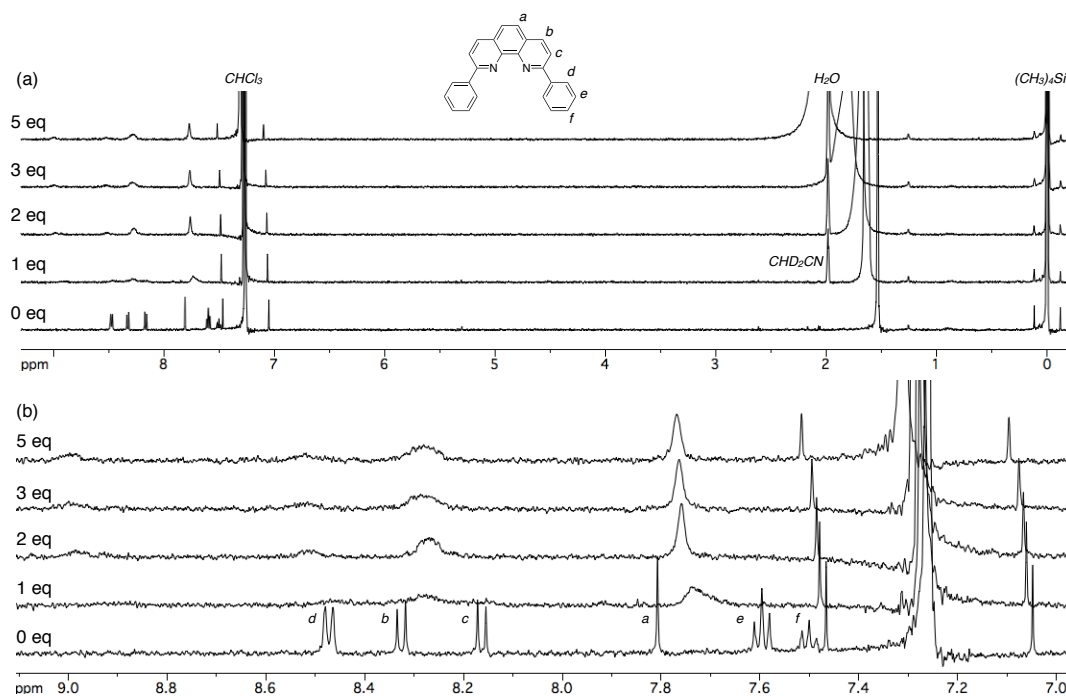


Figure S9.  $^1\text{H}$  NMR spectra (whole region (a) and aromatic region (b)) of **2** with different equivalents of  $\text{HAuCl}_4 \cdot 4\text{H}_2\text{O}$  (500 MHz,  $\text{CDCl}_3$ , 27  $^\circ\text{C}$ ,  $[\mathbf{2}] = 100 \mu\text{M}$ )

#### • UV-vis analysis

A  $\text{CH}_3\text{CN}$  solution of  $\text{HAuCl}_4 \cdot 4\text{H}_2\text{O}$  (1.81 mM) was added stepwise to a solution of **2** (102  $\mu$ M,

1.0 mL, CHCl<sub>3</sub>/CH<sub>3</sub>CN = 10/1), followed by UV-vis absorption measurement. This operation was repeated until a total amount of the added HAuCl<sub>4</sub> reached 2.0 equiv.

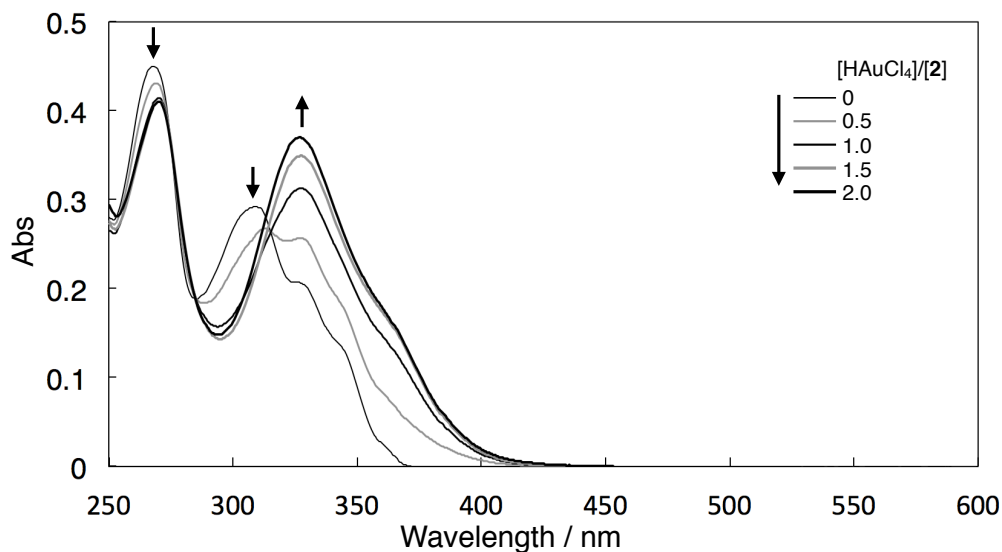


Figure S10. UV-vis spectra of **2** with different equivalents of HAuCl<sub>4</sub>·4H<sub>2</sub>O (CHCl<sub>3</sub>/CH<sub>3</sub>CN = 10/1, 20 °C, [**2**] = 102 μM, *l* = 0.1 cm)

• *Single-crystal XRD analysis*

A single crystal suitable for XRD analysis was obtained as follows. A mixture of **2** (2.3 mg, 6.8 μmol, 1.0 equiv.) in CHCl<sub>3</sub> (300 μL) and HAuCl<sub>4</sub>·4H<sub>2</sub>O (2.8 mg, 6.8 μmol, 1.0 equiv.) in CH<sub>3</sub>CN (100 μL) was filtrated, and diethyl ether was then slowly diffused into the solution for 1 day. The resulting crystals were washed with EtOH (ca. 1 mL × 2) and dried in *vacuo* to afford [H**2**][AuCl<sub>4</sub>] (3.8 mg, 5.6 μmol, 82%) as yellow needles. The structural data were deposited on the CCDC database (CCDC 2017589).

Crystal data for [H**2**][AuCl<sub>4</sub>]: C<sub>24</sub>H<sub>17</sub>Cl<sub>4</sub>AuN<sub>2</sub>, *F*<sub>w</sub> = 672.19, crystal dimensions 0.16 × 0.09 × 0.07 mm, monoclinic, space group *C2/c*, *a* = 23.2563(7), *b* = 8.9664(3), *c* = 22.4002(7) Å, β = 105.104(3)°, *V* = 4509.6(3) Å<sup>3</sup>, *Z* = 8, ρ<sub>calcd</sub> = 1.980 g cm<sup>-3</sup>, μ = 7.036 mm<sup>-1</sup>, *T* = 93 K, λ(MoKα) = 0.71073 Å, 2θ<sub>max</sub> = 55.0°, 17219/4984 reflections collected/unique (*R*<sub>int</sub> = 0.0204), *R*<sub>1</sub> = 0.0173 (*I* > 2σ(*I*)), *wR*<sub>2</sub> = 0.0409 (for all data), GOF = 1.036, largest diff. peak and hole 1.51/−0.83 eÅ<sup>-3</sup>. CCDC deposit number 2017589.

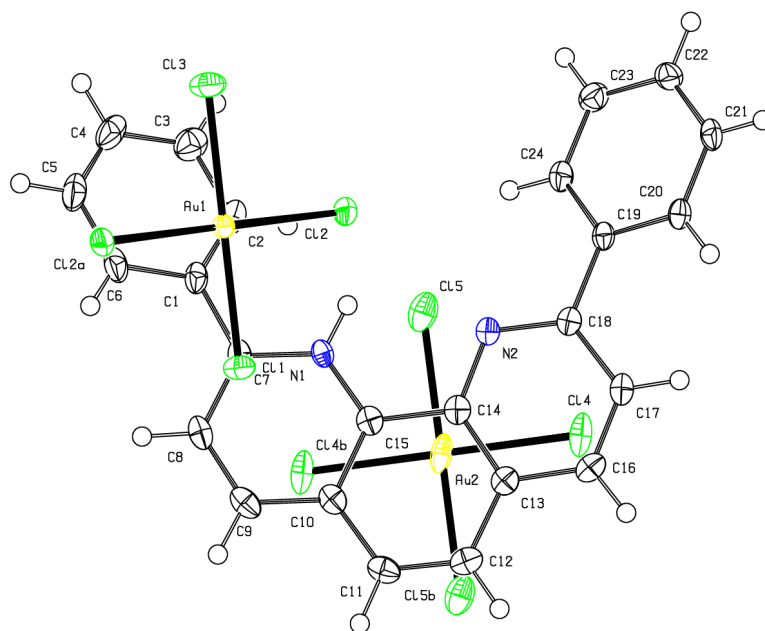


Figure S11. ORTEP drawing of  $[H_2][AuCl_4]$  at the 50% probability level

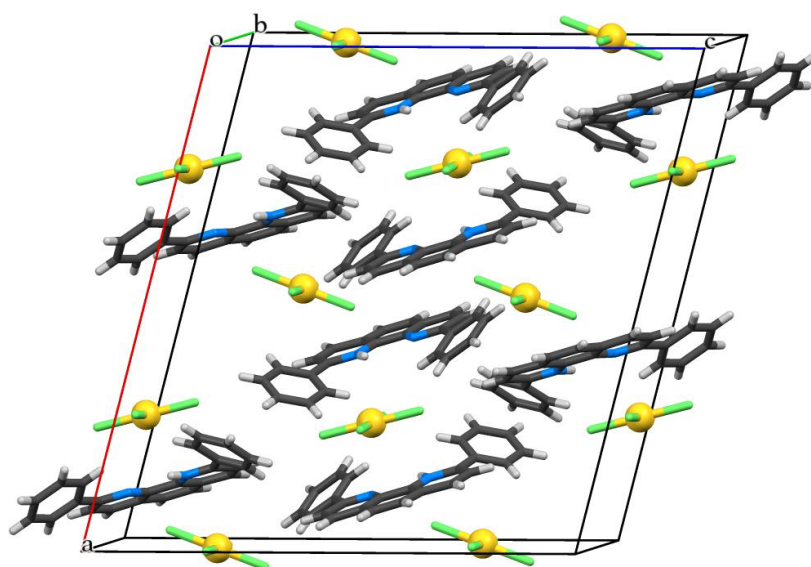


Figure S12. Unit cell structure of  $[H_2][AuCl_4]$  (gray: C, white: H, blue: N, green: Cl, yellow: Au)

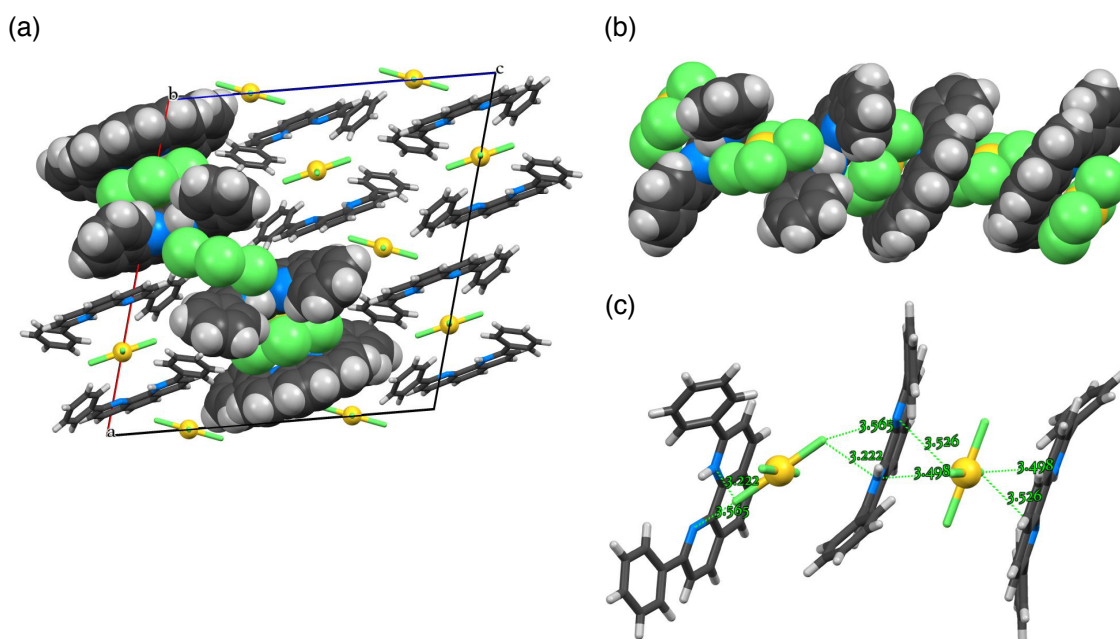


Figure S13. (a) Alternating stacking structure of protonated **2** and  $[\text{AuCl}_4]^-$  in the crystal packing, (b) isolated stacking structure and (c) atom distances between monoprotonated **2** and  $[\text{AuCl}_4]^-$

### **Reaction of 1 and $\text{H}_2\text{PtCl}_6 \cdot 6\text{H}_2\text{O}$**

The concentration of **1** in a solution was determined by  $^1\text{H}$  NMR measurement with anisole as an internal standard. The concentration of  $\text{H}_2\text{PtCl}_6 \cdot 6\text{H}_2\text{O}$  was determined by UV-vis absorption measurement according to a reference ( $\epsilon_{259(\text{water})} = \sim 24,000 \text{ L} \cdot \text{mol}^{-1} \cdot \text{cm}^{-1}$ ).<sup>4</sup>

#### • $^1\text{H}$ NMR analysis

A certain amount of  $\text{H}_2\text{PtCl}_6 \cdot 6\text{H}_2\text{O}$  (200  $\mu\text{M}$ ) in  $\text{CH}_3\text{CN}$  was measured out and evaporated in advance. The resulting solid was added to a solution of **1** (96  $\mu\text{M}$ , 1.0 mL,  $\text{CDCl}_3/\text{CD}_3\text{CN} = 10/1$ , containing 84  $\mu\text{M}$  anisole as an internal standard), followed by  $^1\text{H}$  NMR measurement. This operation was repeated until a total amount of the added  $\text{H}_2\text{PtCl}_6$  reached 2.0 equiv. No signals of cleaved benzyl ether groups of **1** were observed during this experiment, which ensured stability of **1** under this condition even in the presence of 2 equiv. of  $\text{H}_2\text{PtCl}_6$ .

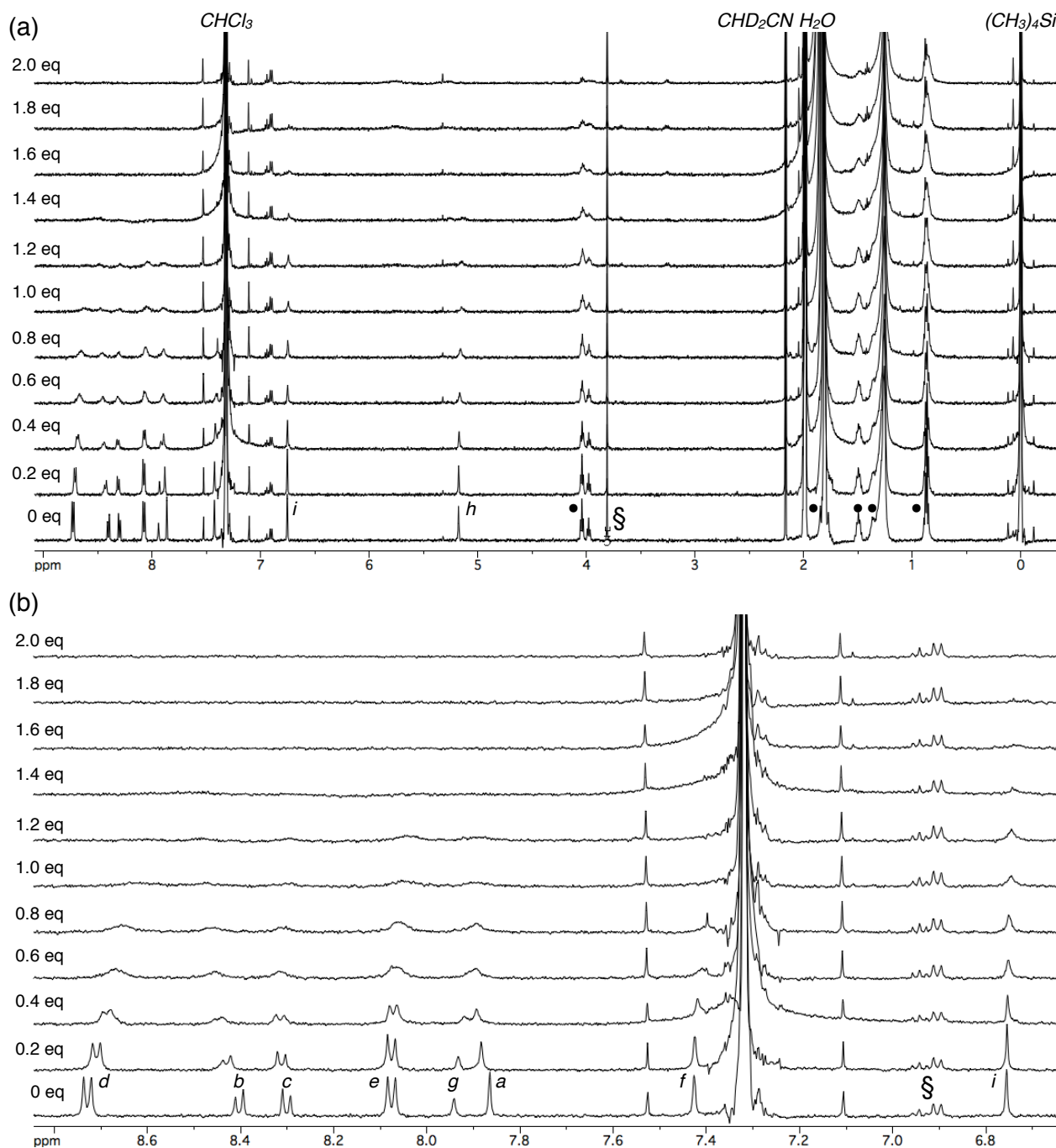
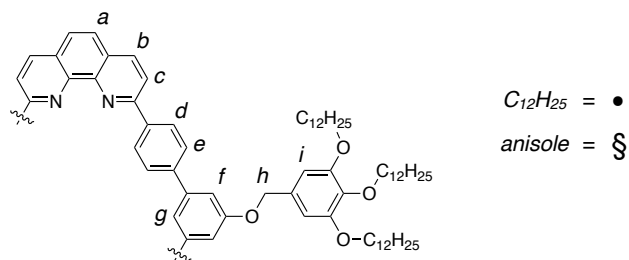


Figure S14.  $^1H$  NMR spectra (whole region (a) and aromatic region (b)) of **1** with different equivalents of  $H_2PtCl_6 \cdot 6H_2O$  (500 MHz,  $CDCl_3/CD_3CN = 10/1$ , 27 °C,  $[1] = 96 \mu M$ , containing anisole as an internal standard)

• *UV-vis analysis*

A certain amount of  $\text{H}_2\text{PtCl}_6 \cdot 6\text{H}_2\text{O}$  ( $200 \mu\text{M}$ ) in  $\text{CH}_3\text{CN}$  was measured out and evaporated in advance. The resulting solid was dissolved in a solution of **1** ( $29 \mu\text{M}$ ,  $2.0 \text{ mL}$ ,  $\text{CHCl}_3/\text{CH}_3\text{CN} = 10/1$ ), followed by UV-vis absorption measurement. This operation was repeated until a total amount of the added  $\text{H}_2\text{PtCl}_6$  reached 3.0 equiv. The significant increase in absorption intensity around 270 nm after adding more than 1.0 equiv. of  $\text{H}_2\text{PtCl}_6$  can be ascribed to the presence of free  $\text{H}_2\text{PtCl}_6$  molecules (Figure S16).

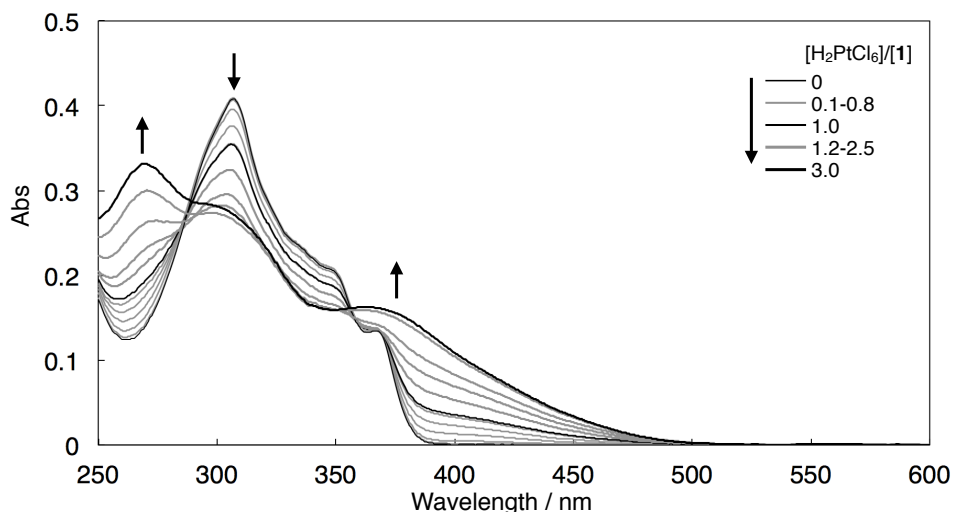


Figure S15. UV-vis spectra of **1** with different equivalents of  $\text{H}_2\text{PtCl}_6 \cdot 6\text{H}_2\text{O}$  ( $\text{CHCl}_3/\text{CH}_3\text{CN} = 10/1$ ,  $20 \text{ }^\circ\text{C}$ ,  $[\mathbf{1}] = 29 \mu\text{M}$ ,  $l = 0.1 \text{ cm}$ )

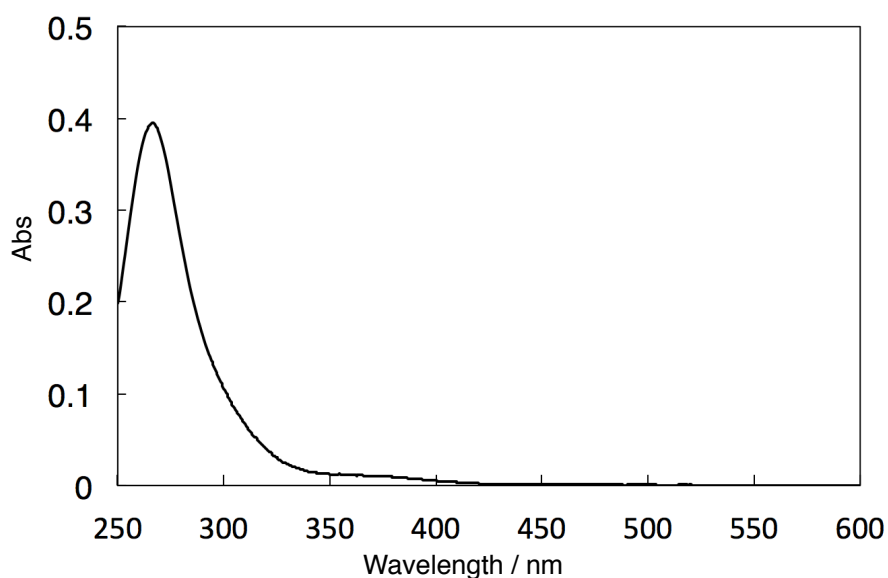


Figure S16. UV-vis spectrum of  $\text{H}_2\text{PtCl}_6 \cdot 6\text{H}_2\text{O}$  ( $\text{CHCl}_3/\text{CH}_3\text{CN} = 10/1$ ,  $20 \text{ }^\circ\text{C}$ ,  $20 \mu\text{M}$ ,  $l = 1 \text{ cm}$ )

- *AFM analysis*

A CH<sub>3</sub>CN solution of H<sub>2</sub>PtCl<sub>6</sub>·6H<sub>2</sub>O (2.03 mM, 21 μL, 1.0 equiv.; 1.72 mM, 21 μL, 2.0 equiv.) was added to a CHCl<sub>3</sub> solution of **1** (84 μM, 500 μL; 90 μM, 200 μL). Right after 10-fold dilution with CHCl<sub>3</sub>/CH<sub>3</sub>CN = 10/1, the solution was spin-coated on mica to conduct AFM measurement.

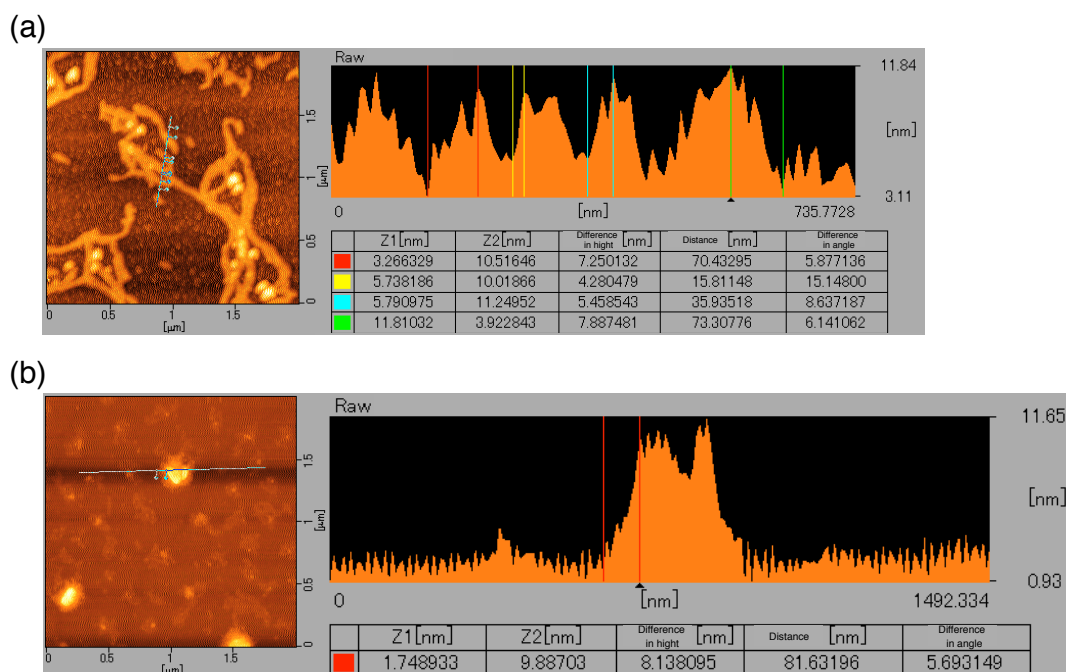


Figure S17. Dry-state AFM images of **1** with (a) 1.0 equiv. or (b) 2.0 equiv. of H<sub>2</sub>PtCl<sub>6</sub>·6H<sub>2</sub>O on mica

- *STEM-EDS analysis*

A CH<sub>3</sub>CN solution of H<sub>2</sub>PtCl<sub>6</sub>·6H<sub>2</sub>O (1.72 mM, 18 μL, 1.0 equiv.) was added to a CHCl<sub>3</sub> solution of **1** (100 μM, 315 μL). Right after 10-fold dilution with CHCl<sub>3</sub>/CH<sub>3</sub>CN = 10/1, the solution was drop-cast on a carbon-coated Cu grid to conduct STEM and EDS measurement.

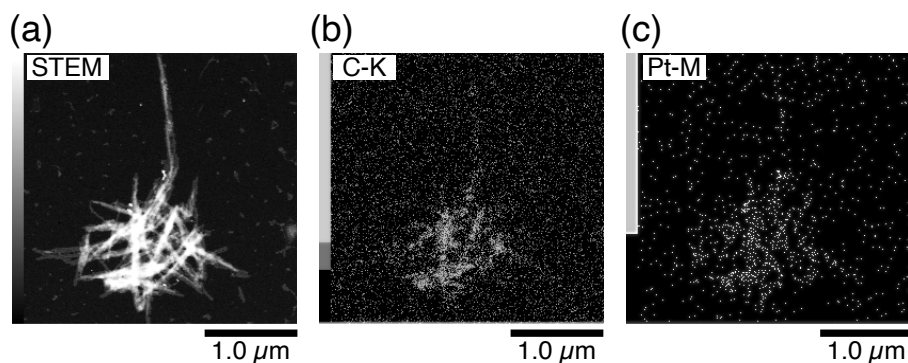


Figure S18. (a) A dark-field STEM image and color-corrected EDS maps for (b) C (K-peak) and (c) Pt (M-peak) of nanofibers composed of **1** and Pt.

## Reaction of 2 and H<sub>2</sub>PtCl<sub>6</sub>·6H<sub>2</sub>O

### • Single-crystal XRD analysis

A single crystal suitable for XRD analysis was obtained as follows. A solution of **2** (2.7 mg, 8.1 μmol, 1.0 equiv.) in CH<sub>3</sub>CN (1 mL) was gently put on a solution of H<sub>2</sub>PtCl<sub>6</sub>·6H<sub>2</sub>O (8.3 mg, 10.2 μmol, 1.3 equiv.) in EtOH (600 μL), which was then allowed to stand for 3 days. The resulting crystals were washed with CH<sub>3</sub>CN (ca. 1 mL × 2) and EtOH (ca. 1 mL), and then dried in *vacuo* to afford [H<sub>2</sub>]<sub>2</sub>[PtCl<sub>6</sub>] (3.2 mg, 2.9 μmol, 73%) as yellow platelet crystals. The structural data were deposited on the CCDC database (CCDC 2017590).

Crystal data for [H<sub>2</sub>]<sub>2</sub>[PtCl<sub>6</sub>]: C<sub>48</sub>H<sub>34</sub>Cl<sub>6</sub>PtN<sub>4</sub>,  $F_w = 1074.63$ , crystal dimensions 0.18 × 0.08 × 0.07 mm, triclinic, space group  $P\bar{1}$ ,  $a = 12.2029(2)$ ,  $b = 13.3559(2)$ ,  $c = 13.8683(2)$  Å,  $\alpha = 80.7745(14)$ ,  $\beta = 67.0066(17)$ ,  $\gamma = 80.4839(16)^\circ$ ,  $V = 2040.61(6)$  Å<sup>3</sup>,  $Z = 2$ ,  $\rho_{\text{calcd}} = 1.749$  g cm<sup>-3</sup>,  $\mu = 3.859$  mm<sup>-1</sup>,  $T = 93$  K,  $\lambda(\text{MoK}\alpha) = 0.71073$  Å,  $2\theta_{\text{max}} = 55.0^\circ$ , 29499/9085 reflections collected/unique ( $R_{\text{int}} = 0.0411$ ),  $R_1 = 0.0260$  ( $I > 2\sigma(I)$ ),  $wR_2 = 0.0544$  (for all data), GOF = 1.035, largest diff. peak and hole 1.08/−1.05 eÅ<sup>-3</sup>. CCDC deposit number 2017590.

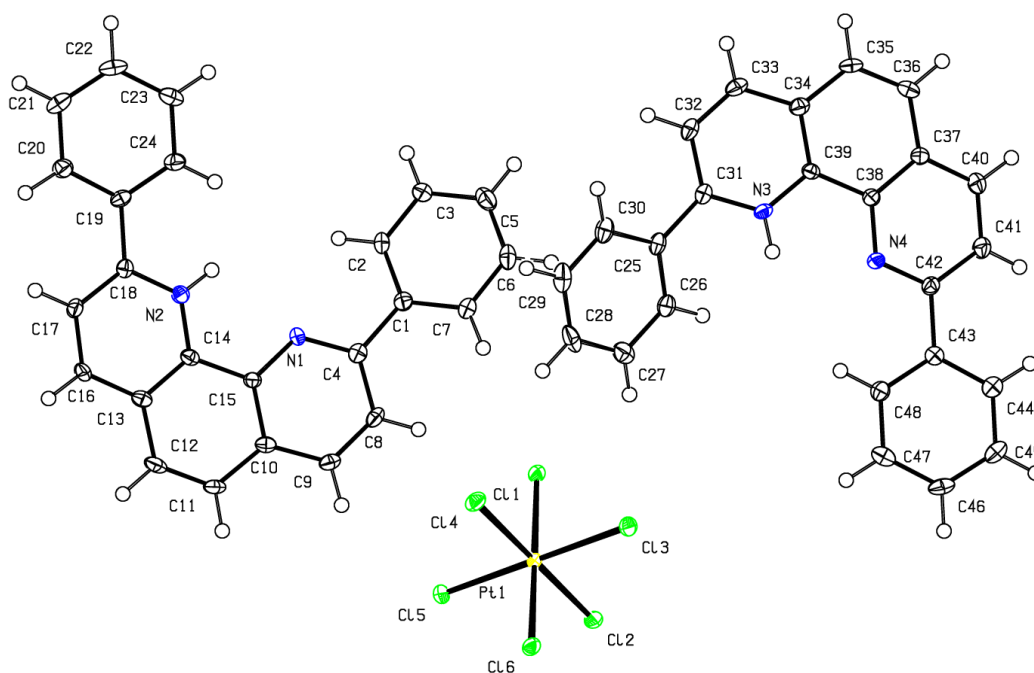


Figure S19. ORTEP drawing of [H<sub>2</sub>]<sub>2</sub>[PtCl<sub>6</sub>] at the 50% probability level

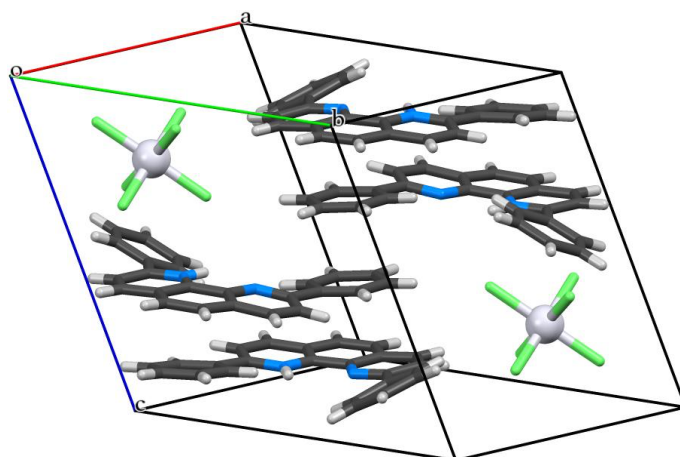


Figure S20. Unit cell structure of  $[\text{H}_2]_2[\text{PtCl}_6]$  (gray: C, white: H, blue: N, green: Cl, silver: Pt)

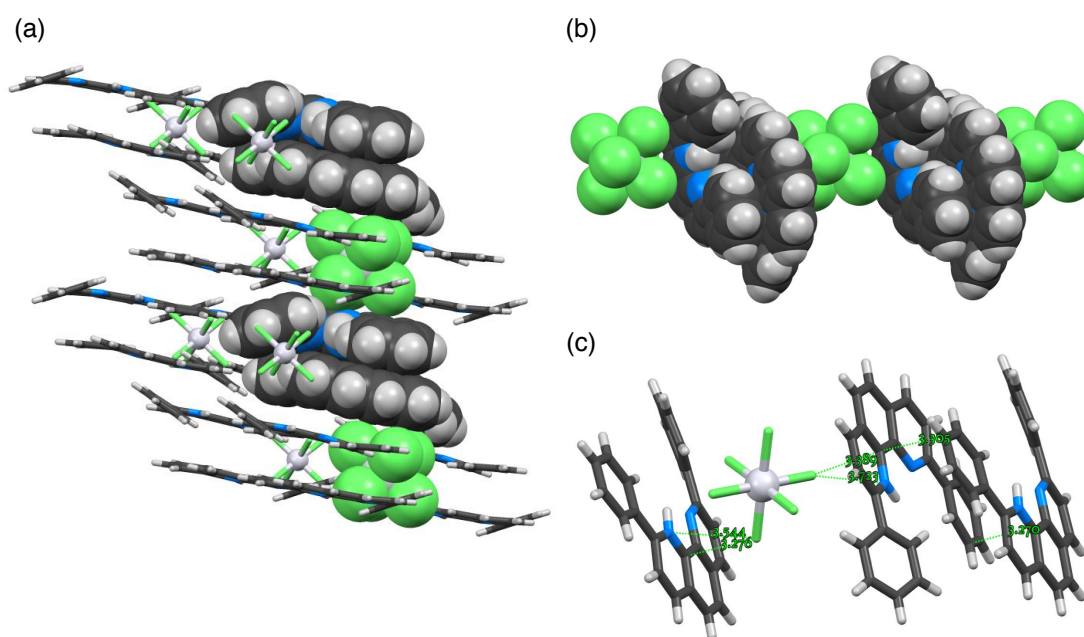


Figure S21. (a) Alternating stacking structure of protonated **2** and  $[\text{PtCl}_6]^{2-}$  in the crystal packing, (b) isolated stacking structure and (c) atom distances between monoprotonated **2** and  $[\text{PtCl}_6]^{2-}$

### **Reaction of 1 and $\text{H}_3\text{PMo}_{12}\text{O}_{40} \cdot n\text{H}_2\text{O}$**

The concentration of **1** in a solution was determined by  $^1\text{H}$  NMR measurement with anisole as an internal standard. The concentration of  $\text{H}_3\text{PMo}_{12}\text{O}_{40} \cdot n\text{H}_2\text{O}$  was determined by UV-vis absorption measurement according to a reference ( $\epsilon_{309.5(\text{MeCN})} = 22,300 \text{ L} \cdot \text{mol}^{-1} \cdot \text{cm}^{-1}$ ).<sup>5</sup>

#### • $^1\text{H}$ NMR analysis

A certain amount of  $\text{H}_3\text{PMo}_{12}\text{O}_{40} \cdot n\text{H}_2\text{O}$  (200  $\mu\text{M}$ ) in  $\text{CH}_3\text{CN}$  was measured out and evaporated in advance. The resulting solid was added to a solution of **1** (96  $\mu\text{M}$ , 1.0 mL,  $\text{CDCl}_3/\text{CD}_3\text{CN} = 10/1$ , containing 84  $\mu\text{M}$  anisole as an internal standard), followed by  $^1\text{H}$  NMR measurement. This operation was repeated until a total amount of the added  $\text{H}_3\text{PMo}_{12}\text{O}_{40}$  reached 1.0 equiv. No signals of cleaved

benzyl ether groups of **1** were observed during this experiment, which ensured stability of **1** under this condition even in the presence of 1 equiv. of  $\text{H}_3\text{PMo}_{12}\text{O}_{40}$ .

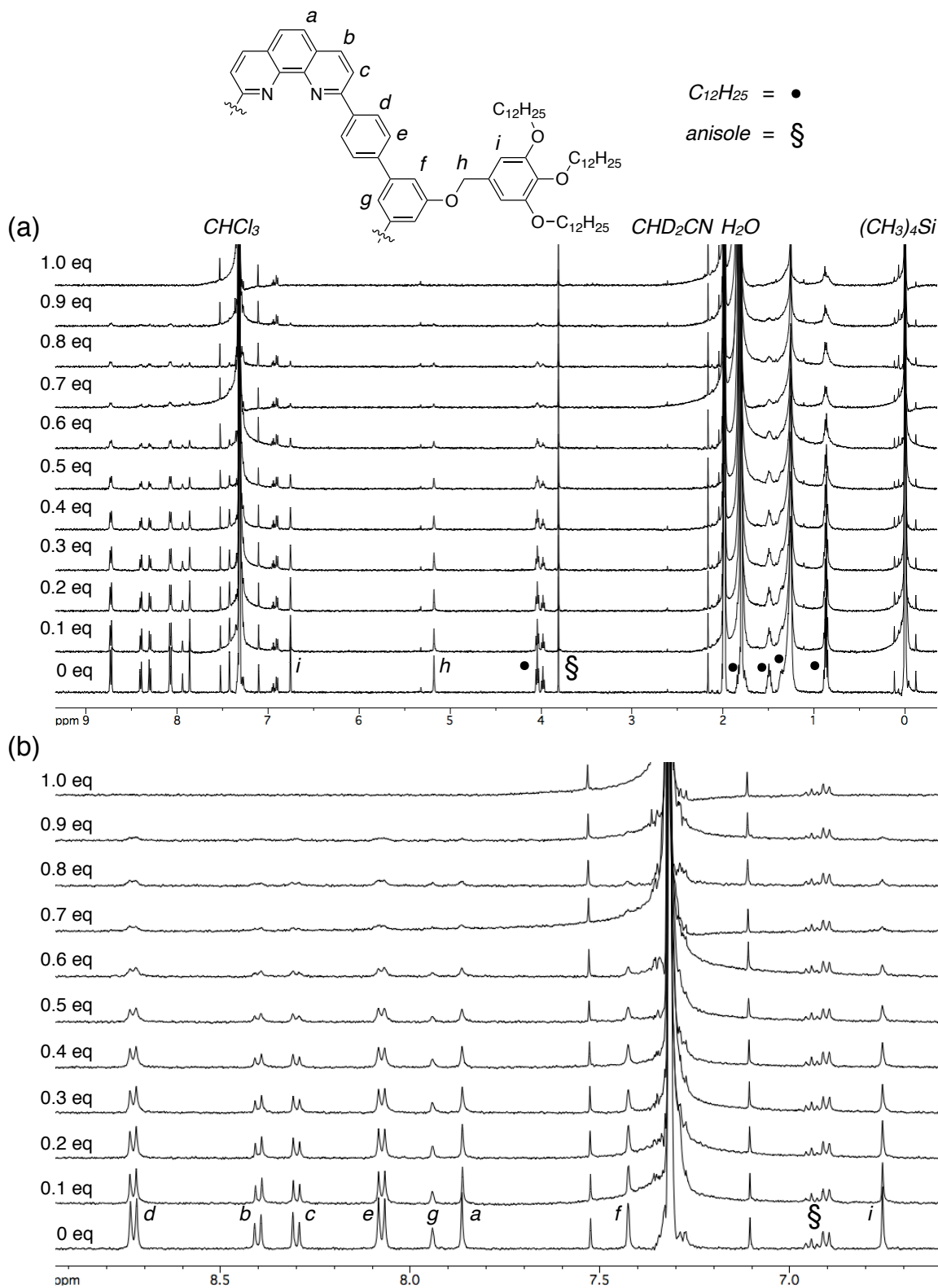


Figure S22.  $^1\text{H}$  NMR spectra (whole region (a) and aromatic region (b)) of **1** with different equivalents of  $\text{H}_3\text{PMo}_{12}\text{O}_{40} \cdot n\text{H}_2\text{O}$  (500 MHz,  $\text{CDCl}_3/\text{CD}_3\text{CN} = 10/1$ ,  $27^\circ\text{C}$ ,  $[\mathbf{1}] = 96 \mu\text{M}$ , containing anisole as an internal standard)

• *UV-vis analysis*

A certain amount of  $\text{H}_3\text{PMo}_{12}\text{O}_{40}\cdot n\text{H}_2\text{O}$  ( $200\ \mu\text{M}$ ) in  $\text{CH}_3\text{CN}$  was measured out evaporated in advance. The resulting solid was dissolved in a solution of **1** ( $29\ \mu\text{M}$ ,  $2.0\ \text{mL}$ ,  $\text{CHCl}_3/\text{CH}_3\text{CN} = 10/1$ ) and UV-vis absorption measurement was then conducted. This operation was repeated until a total amount of the added  $\text{H}_3\text{PMo}_{12}\text{O}_{40}$  reached  $2.0$  equiv. The significant increase in absorption intensity around  $320\ \text{nm}$  after adding more than  $0.8$  equiv. of  $\text{H}_3\text{PMo}_{12}\text{O}_{40}$  can be ascribed to the presence of free  $\text{H}_3\text{PMo}_{12}\text{O}_{40}$  molecules (Figure S24).

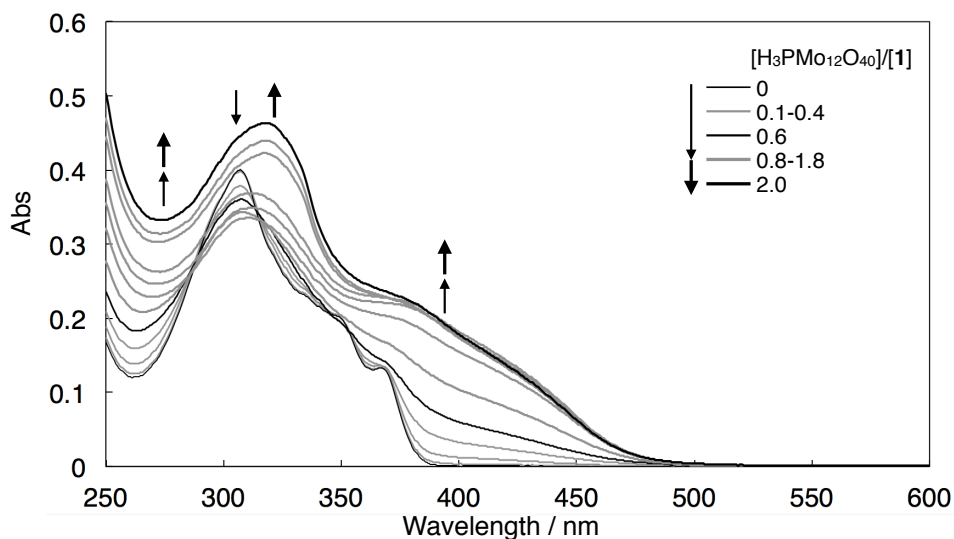


Figure S23. UV-vis spectra of **1** with different equivalents of  $\text{H}_3\text{PMo}_{12}\text{O}_{40}\cdot n\text{H}_2\text{O}$  ( $\text{CHCl}_3/\text{CH}_3\text{CN} = 10/1$ ,  $20\ ^\circ\text{C}$ ,  $[\mathbf{1}] = 29\ \mu\text{M}$ ,  $l = 0.1\ \text{cm}$ )

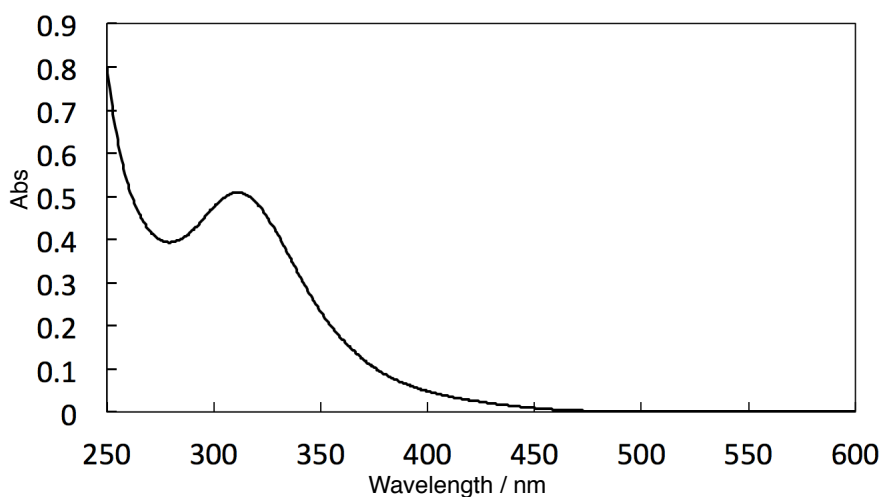


Figure S24. UV-vis spectrum of  $\text{H}_3\text{PMo}_{12}\text{O}_{40}\cdot n\text{H}_2\text{O}$  ( $\text{CHCl}_3/\text{CH}_3\text{CN} = 10/1$ ,  $20\ ^\circ\text{C}$ ,  $21\ \mu\text{M}$ ,  $l = 1\ \text{cm}$ )

- *AFM analysis*

A CH<sub>3</sub>CN solution of H<sub>3</sub>PMo<sub>12</sub>O<sub>40</sub>·*n*H<sub>2</sub>O (2.56 mM, 20 μL, 0.5 equiv.; 2.12 mM, 24 μL, 1.0 equiv.) was added to a CHCl<sub>3</sub> solution of **1** (100 μM, 1000 μL; 102 μM, 500 μL). Right after 10-fold dilution with CHCl<sub>3</sub>/CH<sub>3</sub>CN = 10/1, the solution was spin-coated on mica to conduct AFM measurement.

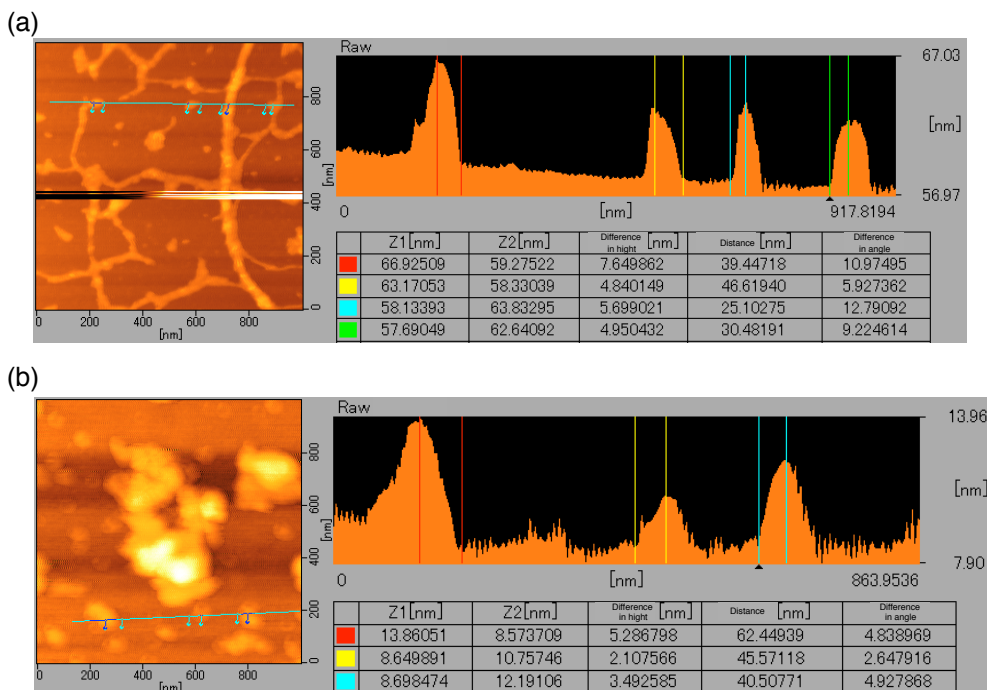


Figure S25. Dry-state AFM images of **1** with (a) 0.5 equiv. or (b) 1.0 equiv. of H<sub>3</sub>PMo<sub>12</sub>O<sub>40</sub>·*n*H<sub>2</sub>O on mica

- *STEM-EDS analysis*

A CH<sub>3</sub>CN solution of H<sub>3</sub>PMo<sub>12</sub>O<sub>40</sub>·*n*H<sub>2</sub>O (536 μM, 100 μL, 5.0 equiv.) was added to a CHCl<sub>3</sub> solution of **1** (109 μM, 1.0 mL). Right after 10-fold dilution with CHCl<sub>3</sub>/CH<sub>3</sub>CN = 10/1, the solution was drop-cast on a carbon-coated Cu grid to conduct STEM and EDS measurement.

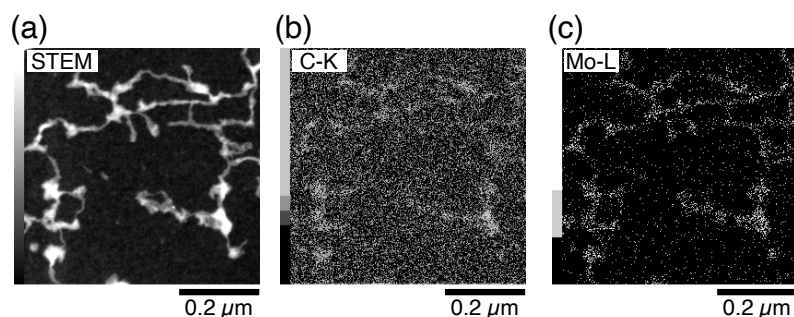


Figure S26. (a) A dark-field STEM image and color-corrected EDS maps for (b) C (K-peak) and (c) Mo (L-peak) of nanofibers composed of **1** and **PMo**.

## Reaction of 2 and H<sub>3</sub>PMo<sub>12</sub>O<sub>40</sub>·nH<sub>2</sub>O

### • Single-crystal XRD analysis

A Single crystal suitable for XRD analysis was obtained as follows. On a solution of **2** (1.0 mg, 3.1 μmol, 1.0 equiv.) in CHCl<sub>3</sub> (400 μL), DMF (100 μL) and a solution of H<sub>3</sub>PMo<sub>12</sub>O<sub>40</sub>·nH<sub>2</sub>O (13.6 mg, 6.2 μmol, 2.0 equiv., assumed *n* = 20) in CH<sub>3</sub>CN (400 μL) were gently added in this order to make a three-layer system composed of CH<sub>3</sub>CN, DMF and CHCl<sub>3</sub> layers, which was then allowed to stand for 1 week. One of the resulting yellow crystals was subjected to single crystal XRD measurement. The structural data were deposited on the CCDC database (CCDC 2017591).

Crystal data for [H<sub>2</sub>]<sub>2</sub>[PMo<sub>12</sub>O<sub>40</sub>][H(DMF)<sub>2</sub>]: C<sub>54</sub>H<sub>49</sub>Mo<sub>12</sub>N<sub>6</sub>O<sub>42</sub>P, *F*<sub>w</sub> = 2636.24, crystal dimensions 0.440 × 0.230 × 0.180 mm, triclinic, space group *P*1, *a* = 12.24560(12), *b* = 12.33600(15), *c* = 13.69940(18) Å, α = 115.9800(12), β = 95.1937(9), γ = 102.8330(9)°, *V* = 1771.73(4) Å<sup>3</sup>, *Z* = 1, ρ<sub>calcd</sub> = 2.471 g cm<sup>-3</sup>, μ = 2.172 mm<sup>-1</sup>, *T* = 93 K, λ(MoKα) = 0.71073 Å, 2θ<sub>max</sub> = 55.0°, 43488/16131 reflections collected/unique (*R*<sub>int</sub> = 0.0168), *R*<sub>1</sub> = 0.0329 (*I* > 2σ(*I*)), *wR*<sub>2</sub> = 0.0843 (for all data), GOF = 1.033, largest diff. peak and hole 2.14/−1.38 eÅ<sup>-3</sup>, Flack parameter = 0.25(2). CCDC deposit number 2017591.

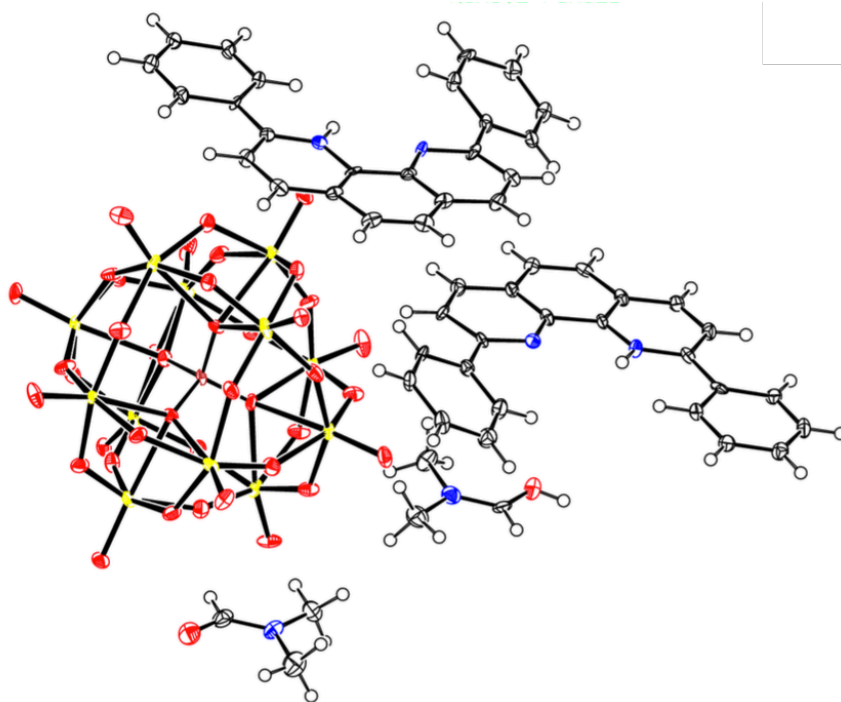


Figure S27. ORTEP drawing of [H<sub>2</sub>]<sub>2</sub>[PMo<sub>12</sub>O<sub>40</sub>][H(DMF)<sub>2</sub>] at the 50% probability level

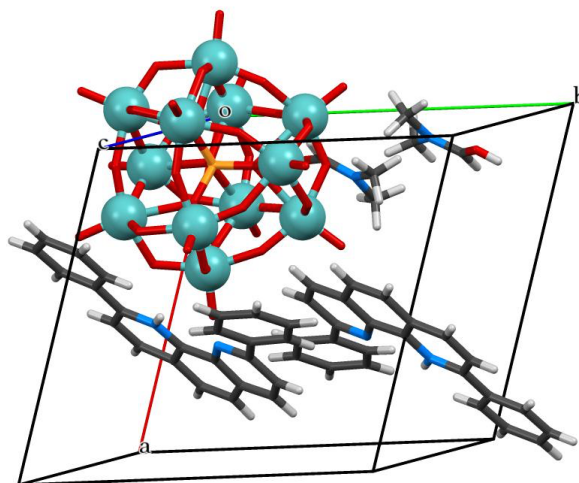


Figure S28. Unit cell structure of  $[\text{H}_2]_2[\text{PMo}_{12}\text{O}_{40}][\text{H}(\text{DMF})_2]$  (gray: C, white: H, blue: N, red: O, orange: P, moss green: Mo)

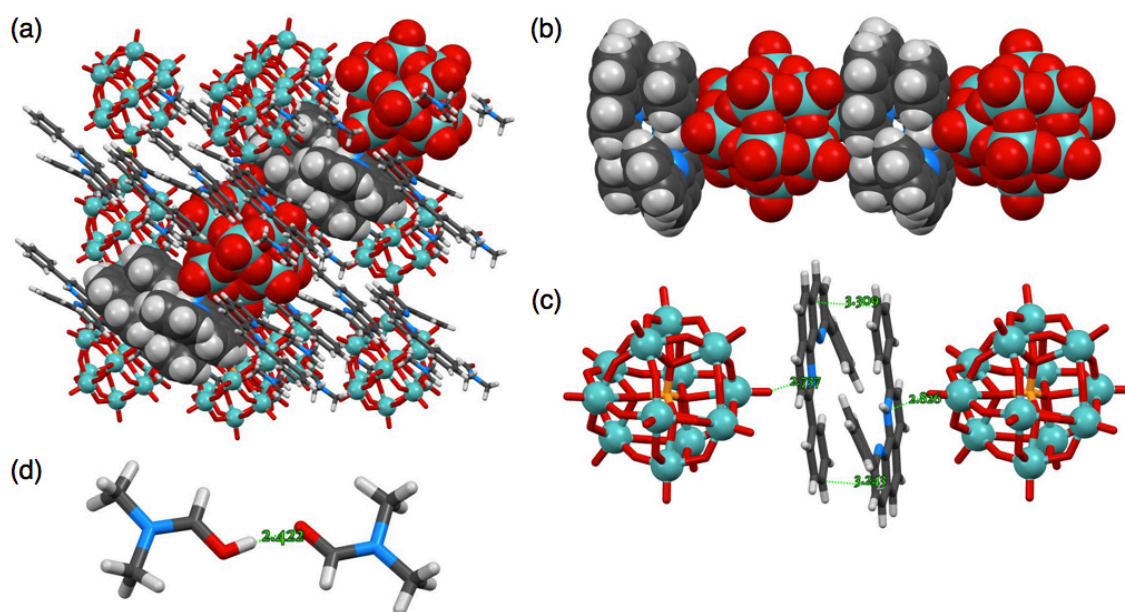


Figure S29. (a) Alternating stacking structure of protonated **2** and  $[\text{PMo}_{12}\text{O}_{40}]^{3-}$  in the crystal packing, (b) isolated stacking structure, (c) atom distances between monoprotonated **2** and  $[\text{PMo}_{12}\text{O}_{40}]^{3-}$  and (d) monoprotonated DMF dimer

### **Reduction of nanofibers composed of 1 and $\text{HAuCl}_4 \cdot 4\text{H}_2\text{O}$**

#### ***• Synthesis and UV-vis analysis***

To a solution of **1** (139  $\mu\text{M}$ , 1.0 mL, 1.0 equiv.) in  $\text{CHCl}_3/\text{CH}_3\text{CN}$  (10:1) was added a  $\text{CH}_3\text{CN}$  solution of  $\text{HAuCl}_4 \cdot 4\text{H}_2\text{O}$  (2.07 mM, 134  $\mu\text{L}$ , 2.0 equiv.). After stirring for 30 min, an aqueous solution of  $\text{NaBH}_4$  (60 mM, 23  $\mu\text{L}$ , 10 equiv.) was rapidly added to the reaction mixture under vigorous stirring. After stirring for 3 h, the purple organic layer was evaporated under reduced pressure to afford purple powder. The resulting solid was dissolved in  $\text{CHCl}_3$  (1.0 mL) and UV-vis

was then measured.

- *STEM-EDS analysis*

Reduction of tetrachloroaurate-assembling nanofibers was performed in the same procedure using **1** (315  $\mu\text{M}$ , 1.0 mL, 1.0 equiv.),  $\text{HAuCl}_4 \cdot 4\text{H}_2\text{O}$  (19.3 mM, 33  $\mu\text{L}$ , 2.0 equiv.) and  $\text{NaBH}_4$  (82 mM, 38  $\mu\text{L}$ , 10 equiv.). The resulting solid was dissolved in  $\text{CHCl}_3/\text{CH}_3\text{CN} = 10/1$  (10  $\mu\text{M}$ ) and drop-cast on a carbon-coated Cu grid to conduct STEM and EDS measurement.

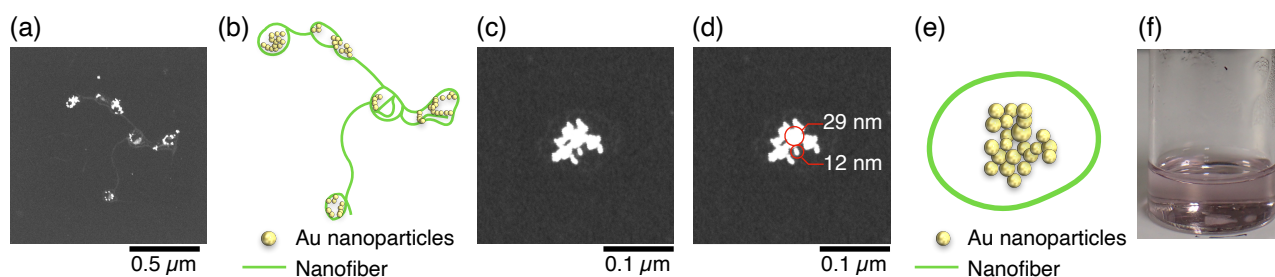


Figure S30. (a),(b) A dark-field STEM image of the resulting gold nanoparticles and its schematic representation, respectively. (c),(d),(e) A dark-field STEM image focused on one aggregate of gold nanoparticles, diameters of selected nanoparticles, and its schematic representation, respectively. (d) Picture of the sample ( $1/\text{Au} = 1:2$ ) reduced by  $\text{NaBH}_4$  and subsequently re-dissolved in  $\text{CHCl}_3$ .

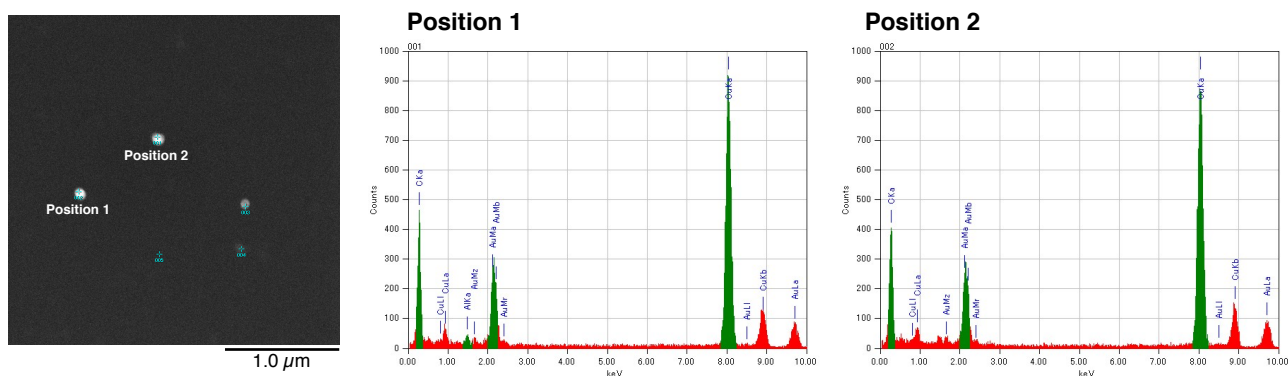


Figure S31. STEM images (dry-state) of gold nanoparticles obtained by reduction of tetrachloroaurate-assembled nanofibers and EDS analyses at two positions

### **Reduction of nanofibers composed of **1** and $\text{H}_3\text{PMo}_{12}\text{O}_{40} \cdot n\text{H}_2\text{O}$**

- *Synthesis, UV-vis and AFM analysis*

An aqueous solution of L-ascorbic acid (356  $\mu\text{M}$ , 270  $\mu\text{L}$ , 3.0 equiv.) was measured out and the solvent was evaporated under reduced pressure in advance. To the resulting solid was added a mixture of **1** (82  $\mu\text{M}$ , 1.7 equiv.) and  $\text{H}_3\text{PMo}_{12}\text{O}_{40} \cdot n\text{H}_2\text{O}$  (49  $\mu\text{M}$ ) in  $\text{CHCl}_3/\text{CH}_3\text{CN} = 5.3:1$  (660  $\mu\text{L}$ ).

The mixture was allowed to stand at room temperature for 24 h in the dark, followed by UV-vis absorption measurement. A similarly prepared mixture was diluted to 10  $\mu$ M with CHCl<sub>3</sub>/CH<sub>3</sub>CN (10:1) and spin-coated on mica to conduct AFM measurement.

## **References**

1. M. Kuritani, S. Tashiro and M. Shionoya, *Chem. Asian J.*, 2013, **8**, 1368–1371.
2. G. M. Sheldrick, *SHELXL-97, Program for refinement of crystal structure* (University of Göttingen, Göttingen, Germany, 1997); *SHELXL-2013* (University of Göttingen, Göttingen, Germany, 2013).
3. V. Soni, R. S. Sindal and R. N. Mehrotra, *Inorg. Chim. Acta*, 2007, **360**, 3141–3148.
4. G. Holzner, F. H. Kriel and C. Priest, *Anal. Chem.*, 2015, **87**, 4757–4764.
5. K. Nomiya, Y. Sugie, K. Amimoto and M. Miwa, *Polyhedron*, 1987, **6**, 519–524.